

# FREQUENCY MAP ANALYSIS AND PARTICLE ACCELERATORS

J.Laskar

Astronomie et Systèmes Dynamiques, CNRS-UMR8028, IMCCE-Observatoire de Paris,  
77 Av Denfert-Rochereau, 75014 Paris

## Abstract

The development of frequency map analysis in particle accelerators is reviewed. In many examples, the frequency map is folded at large amplitudes. The fold is a singularity in the frequency map that induces a change of the signature of the torsion. When the torsion is non definite, the dynamical behavior of the beam needs to be studied very precisely, as directions of fast escape may occur.

## INTRODUCTION

Frequency map analysis (FMA) was introduced for the demonstration and understanding of the chaotic behavior of the Solar System [1], that can be considered as a dynamical system with  $3N$  degrees of freedom (DOF), where  $N$  is the number of the planets. The method applies more generally to any Hamiltonian system or symplectic map (eventually with some small dissipation) [2, 3, 4]. It is particularly interesting for systems of DOF larger than 2, when a simple surface of section fails to provided a global view of the dynamics of the system. FMA is now largely used, from studies on atomic physics [5] to galactic dynamics [6, 7, 8, 9, 10]. The application to particle accelerator dynamics was very natural [11], as the motion of a single particle in a storage ring is usually described in a surface of section of the beam by a symplectic map of dimension 4, or eventually of dimension 6 when the synchrotron oscillation is also taken into account. Since, FMA has been applied to many machines, providing in each case a picture ID of the dynamics of the beam [12, 13, 14, 15, 16, 17]. Reviews of the method with demonstrations of its convergence for regular trajectories can be found in [18, 19, 20]. Here, after a brief recall of the main aspects of FMA, we will focus on the implications of folds that appear in several examples of frequency maps.

## FREQUENCY MAPS

Although FMA is not a perturbative theory, it is useful to describe its properties for a Hamiltonian close to integrable, where a rigorous setting can be derived. Let us thus consider a  $n$ -DOF Hamiltonian system in the form  $H(I, \theta) = H_0(I) + \varepsilon H_1(I, \theta)$ , where  $H$  is real analytic for canonical variables  $(I, \theta) \in B^n \times \mathbb{T}^n$ ,  $B^n$  is a domain of  $\mathbb{R}^n$  and  $\mathbb{T}^n$  is the  $n$ -dimensional torus. For  $\varepsilon = 0$ , the Hamiltonian reduces to  $H_0(I)$  and is integrable. The equa-

tions of motion are then for all  $j = 1, \dots, n$

$$\dot{I}_j = 0, \quad \dot{\theta}_j = \frac{\partial H_0(I)}{\partial I_j} = \nu_j(I); \quad (1)$$

The motion in phase space takes place on tori, products of circles with radii  $I_j$ , which are described at constant velocity  $\nu_j(I)$ . If the system is nondegenerate, that is if

$$\det \left( \frac{\partial \nu(I)}{\partial I} \right) = \det \left( \frac{\partial^2 H_0(I)}{\partial I^2} \right) \neq 0 \quad (2)$$

the frequency map

$$F : \mathbb{B}^n \longrightarrow \mathbb{R}^n \\ (I) \longrightarrow (\nu) \quad (3)$$

is a diffeomorphism (one to one smooth map) on its image  $\Omega$ , and the tori are as well described by the action variables  $(I) \in B^n$  or by the frequency vector  $(\nu) \in \Omega$ . For a nondegenerate system, KAM theorem [21] still asserts that for sufficiently small values of  $\varepsilon$ , there exists a Cantor set  $\Omega_\varepsilon$  of values of  $(\nu)$ , satisfying a Diophantine condition of the form

$$|\langle k, \nu \rangle| = |k_1 \nu_1 + \dots + k_n \nu_n| > \kappa_\varepsilon / |k|^m \quad (4)$$

for which the perturbed system still possesses smooth invariant tori with linear flow (the KAM tori). Moreover, these tori that survive on a totally discontinuous set of initial conditions are still properly ordered in some sense as, according to Pöschel [22], there exists a diffeomorphism

$$\Psi : \mathbb{T}^n \times \Omega \longrightarrow \mathbb{T}^n \times B^n; \quad (\varphi, \nu) \longrightarrow (\theta, I) \quad (5)$$

which is analytical with respect to  $\varphi$ ,  $C^\infty$  in  $\nu$ , and on  $\mathbb{T}^n \times \Omega_\varepsilon$  transforms the Hamiltonian equations into the trivial system

$$\dot{\nu}_j = 0, \quad \dot{\varphi}_j = \nu_j. \quad (6)$$

If we fix  $\theta \in \mathbb{T}^n$  to some value  $\theta = \theta_0$ , we obtain a frequency map on  $B^n$  defined as

$$F_{\theta_0} : B^n \longrightarrow \Omega \\ I \longrightarrow (\nu) = p_2(\Psi^{-1}(\theta_0, I)) \quad (7)$$

where  $p_2$  is the projection on  $\Omega$  ( $p_2(\phi, \nu) = \nu$ ). For sufficiently small  $\varepsilon$ , the torsion condition (2) ensures that the frequency map  $F_{\theta_0}$  is still a smooth diffeomorphism.

## FREQUENCY MAP ANALYSIS

The FMA method relies heavily on the observation that when a quasiperiodic function  $f(t)$  is given numerically over a finite time span  $[-T, T]$ , it is possible to recover its fundamental frequencies in a very precise way, several orders of magnitude more precisely than by simple Fourier analysis. Indeed, let

$$f(t) = e^{i\nu_1 t} + \sum_{k \in \mathbb{Z}^n - (1, 0, \dots, 0)} a_k e^{i\langle k, \nu \rangle t}, \quad a_k \in \mathbb{C} \quad (8)$$

be a KAM quasiperiodic solution of our Hamiltonian system, where the frequency vector ( $\nu$ ) satisfies a Diophantine condition (4). The frequency analysis algorithm NAFF will provide an approximation  $f'(t) = \sum_{k=1}^N a_k e^{i\omega_k t}$  of  $f(t)$  from its numerical knowledge over a finite time span  $[-T, T]$ . The frequencies  $\omega_k$  and complex amplitudes  $a_k$  are computed through an iterative scheme. In order to determine the first frequency  $\omega_1$ , one searches for the maximum amplitude of  $\phi(\sigma) = \langle f(t), e^{i\sigma t} \rangle$  where the scalar product  $\langle f(t), g(t) \rangle$  is defined by

$$\langle f(t), g(t) \rangle = \frac{1}{2T} \int_{-T}^T f(t) \bar{g}(t) \chi(t) dt, \quad (9)$$

and where  $\chi(t)$  is a weight function. Once the first periodic term  $e^{i\omega_1 t}$  is found, its complex amplitude  $a_1$  is obtained by orthogonal projection, and the process is restarted on the remaining part of the function  $f_1(t) = f(t) - a_1 e^{i\omega_1 t}$ . For a KAM quasiperiodic solution (8), the computed frequency  $\nu_1^T$  converges very rapidly towards the true frequency  $\nu_1$  as [19, 20]

$$\nu_1 - \nu_1^T = O\left(\frac{1}{T^{2p+2}}\right) \quad (10)$$

where  $p$  is the order of the cosine window  $\chi_p(t) = 2^p (p!)^2 (1 + \cos \pi t)^p / (2p)!$  used in (9). To construct numerically a frequency map, we will fix all initial angles  $\theta_i = \theta_{i0}$ , and for each initial action values  $(I) = (I_1, \dots, I_n)$ , integrate numerically the trajectories over a finite time interval of length  $T$ . The fundamental frequencies ( $\nu$ ) are computed by the previous (NAFF) algorithm, for all initial actions  $(I)$ , and we thus construct a correspondence :

$$\begin{aligned} F_{\theta_0}^T : B^n &\longrightarrow \Omega \\ I &\longrightarrow (\nu) \end{aligned} \quad (11)$$

that converges towards  $F_{\theta_0}$  as  $T \longrightarrow +\infty$ . This map will thus be regular on the set of regular trajectories, and whenever it appears to be non regular, it will reveal the existence of chaotic orbits (see [3, 18, 19] for more details). In practice, to study the dynamics of a beam, in a given surface of section corresponding to a starting location on the lattice, one can fix the two transverse momenta, and integrate the trajectories with a tracking code for a network of initial conditions spanning both horizontal and vertical directions (Fig.1).

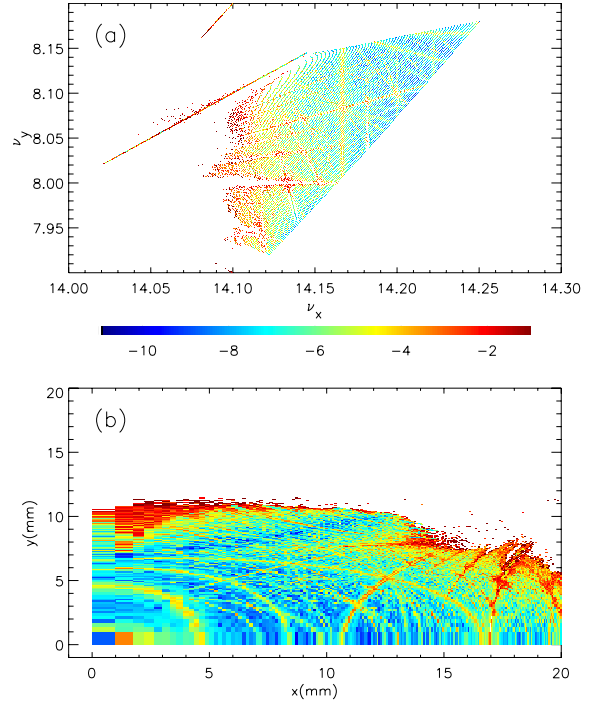


Figure 1: Frequency map for an ideal lattice of the ALS. The initial conditions are taken over a mesh in the horizontal ( $x$ ) and vertical direction ( $y$ ) (bottom), and the corresponding frequencies are plotted in the frequency plane (top). The color indicates the regularity of the orbits : from blue (very regular), to red (very chaotic), while the absence of a dot means that the particle escaped. This allows to easily relate the resonant features observed in the frequency space to regions of the physical space [11, 12, 16]

## EXPERIMENTAL FREQUENCY MAPS

The first frequency maps that were made [11] used numerical models of an ideal lattice (Fig.1). But errors in the magnets, misalignments, and all breakings of the lattice symmetry will in general reduce considerably the stable part of the beam by increasing the strength of the nonlinearities and number of dangerous resonances. A large effort has been made at the ALS to measure precisely these defects [23] and the resulting frequency map provides a more realistic vision of the current machine [12, 13, 17]. Nevertheless, the most critical way to check the real dynamical behavior of a beam remains the construction of an experimental frequency map [24, 25, 13, 26].

In order to realize such a map, fast pinger magnets are used to kick the beam horizontally and vertically in order to span the phase space in both directions. The beam position is recorded using turn by turn beam position monitors, and the resulting data is analyzed using frequency analysis algorithms. The first complete experimental frequency map was realized at the ALS (Fig.2), probing the importance of coupling resonances of high order in the actual behavior of the beam, with an amazing agreement with the numerical model [13].

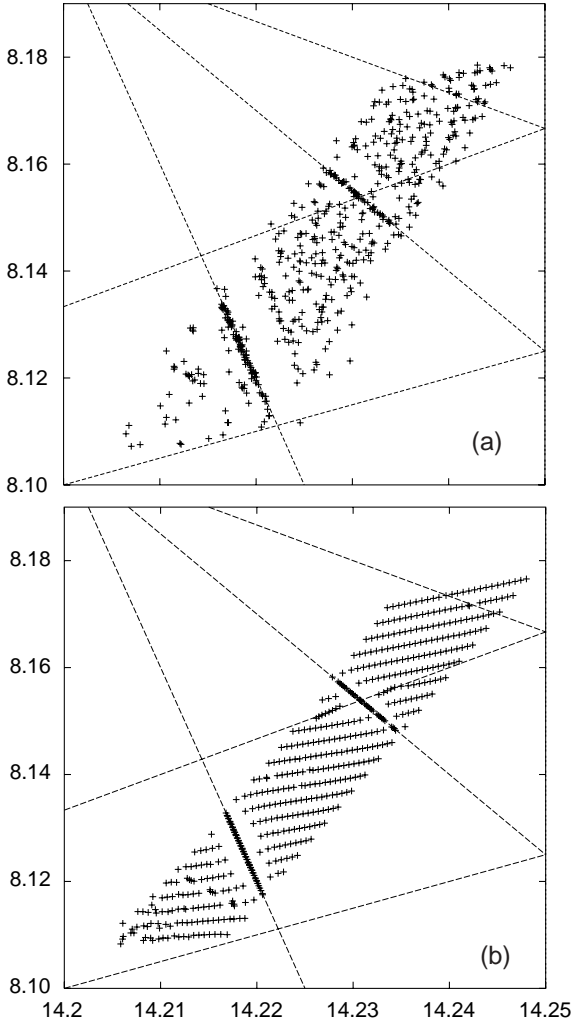


Figure 2: Experimental frequency map (a), and numerical simulation (b) for the ALS with its current settings. Resonances of order  $\leq 5$  are plotted with dotted lines [13].

## FOLDED FREQUENCY MAPS

In several examples, the frequency map appears to be folded. This occurs when the terms of higher degrees in the Hamiltonian become dominant over the quadratic terms as the amplitude increases [15, 27, 17]. Sometimes this occurs as the sextupoles strength have been adjusted in order to avoid some resonant lines that are thought to be dangerous, or merely as the result of beam-beam interactions [15] (Fig. 3). In order to better understand the implications of this folded map, we need to look more closely to the torsion.

The torsion matrix (a generalization of tune-shift with amplitude), is defined as the Jacobian matrix

$$M = \left( \frac{\partial \nu(I)}{\partial I} \right) \approx \left( \frac{\partial^2 H_0(I)}{\partial I^2} \right) \quad (12)$$

If we remove the linear terms of the Hamiltonians by a proper change of variable, and limit its expansion to the

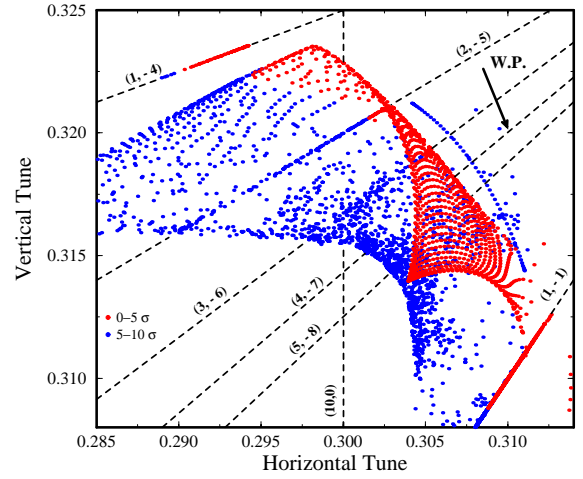


Figure 3: Frequency map of a beam-beam interaction simulation for the LHC [15].

lower orders, the Hamiltonian becomes

$$H = \frac{1}{2} I^T M I + o(I^2) + O(\varepsilon), \quad (13)$$

where  $I^T$  is the transpose of  $I$ . For a fixed energy value  $h$ , even in presence of chaotic diffusion, the variations of the actions will thus be limited by  $I^T M I \approx 2h = Cte$ , and in an equivalent way, when considering the frequencies,  $(\nu) \approx M \times (I)$ , the diffusion of the frequencies will fulfill

$$\nu^T M^{-1} \nu \approx 2h = Cte \quad (14)$$

where  $M^{-1}$  is a symmetric  $2 \times 2$  matrix for a typical accelerator dynamics, when the synchrotron oscillation is neglected. It is known that when the torsion  $M$  is the matrix of a definite quadratic form, finite time stability results exist, that do not persist in case of non definite torsion [28]. This can be understood as in case of non-definite torsion, the isotropic directions of the quadratic form  $M$  will lead to directions of fast escape :

Let  $M^{-1} = \begin{pmatrix} a & c \\ c & b \end{pmatrix}$ . The vector  $V = (x, y)$  is an isotropic direction if  $V^T M^{-1} V = ax^2 + 2cxy + by^2 = 0$ . The discriminant of this equation in  $x$  is  $\Delta = y^2(c^2 - ab) = -y^2 \det(M^{-1})$ . Thus, if  $\det(M) > 0$ , we have  $\Delta < 0$  : the quadratic form is definite and there are no isotropic directions. On the contrary, when  $\det(M) < 0$ ,  $\Delta > 0$  and there are 2 isotropic directions, that will act as asymptotes for the diffusion of the frequencies. The different behavior of the diffusion for definite or non definite torsion is illustrated in Figs. 4a,b. In both figures, the dynamical system is very similar but Fig.4a will correspond to a quadratic Hamiltonian of the form  $H_+ \approx I_1^2 + I_2^2$ , while Fig.4b has non definite torsion ( $H_- \approx I_1^2 - I_2^2$ ). The chaotic zones are very similar, but for  $H_+$ , the trajectories remain bounded over  $10^7$  iterations while for  $H_-$  the resonance 1 : 1 is a direction of fast escape, as the motion of the frequencies

tend to bring them closer to this resonance line while for  $H_+$  the diffusion of the frequencies tends to make them escape the resonance.

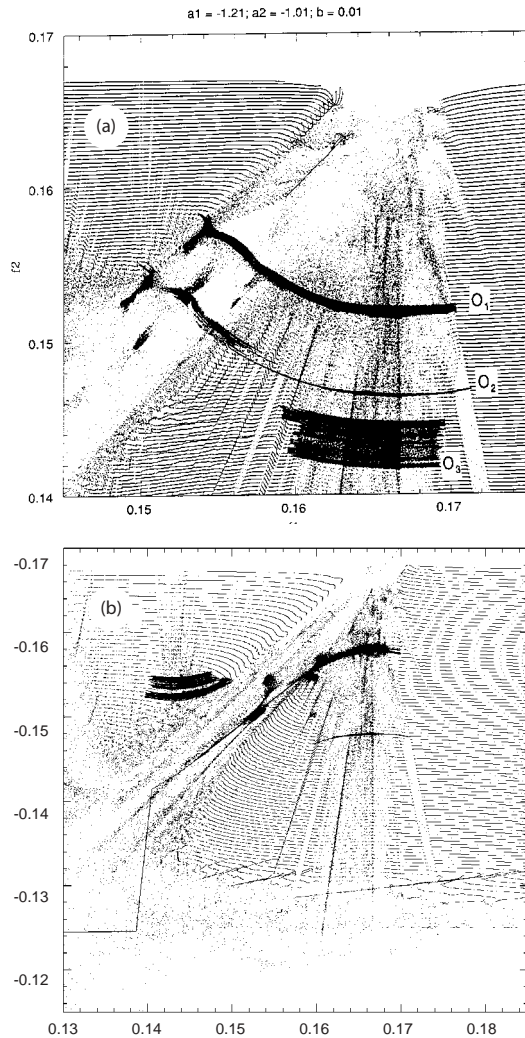


Figure 4: (a) Diffusion of the orbits in a symplectic map of dimension 4 with definite torsion. The background is the image by the frequency map of a regular mesh of initial conditions in the action plane, obtained with only 500 iterations, while the three trajectories  $O_1, O_2, O_3$  are obtained by following the frequencies over  $10^7$  turns, and reveal the actual diffusion of the chaotic trajectories in the frequency plane. [3]. (b) Diffusion with non definite torsion. The dynamical system is similar as in figure 4a, but the system has now non definite torsion. The chaotic trajectories in the frequency plane now follows hyperbolic trajectories, with occasionally a fast direction of escape (here the resonance (1:1)) [19].

### Folded maps

As the signature of the torsion is associated to the determinant of the Jacobian matrix, it becomes easy to under-

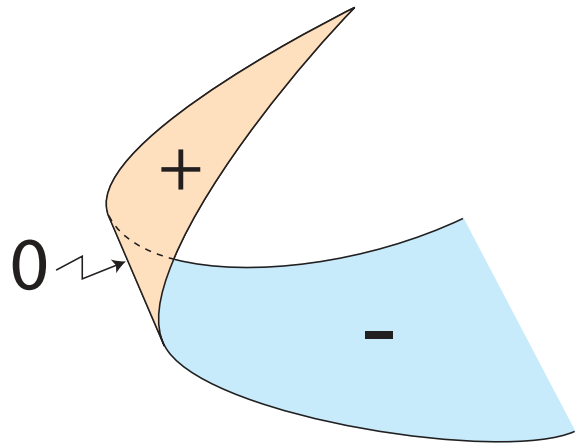


Figure 5: folded frequency map. The determinant of the torsion matrix is zero on the fold, and its sign changes on each side of the fold, as well as the signature of the torsion.

stand the torsion behavior for a 2-dimensional frequency map. First let us recall that for a  $\mathbb{R}^2 \rightarrow \mathbb{R}^2$  map, the only singularities that generically occur are folds or cusps [29]. In all cases, the folds correspond to locations where the determinant of the Jacobian matrix  $M$  is null. If the torsion is definite in the center part of the beam, as required to ensure its maximum stability, the torsion will become non-definite after the fold which can lead to directions of fast diffusion (Fig.5). One should thus analyze very carefully the dynamical behavior after a fold. If the trajectories in the considered region are very regular, no significant diffusion will occur, and there may also be small chaotic regions where the diffusion is limited by the presence of neighboring regular regions, as in figure 4b, but one needs to check very carefully that no region of fast escape (as the 1:1 resonance in Fig. 4b) are present in the operating condition of the machine.

In fact, if there are directions of fast escape, these may be detected with traditional tracking of the particles, but in cases of a double folded frequency map (Fig.6), the tracking may not reveal any escape, as the possible unstable orbits resulting from non-definite torsion are still bounded by the region of definite torsion that lays after the second fold. One should be aware that these designs are potentially very unstable. Indeed, in a real machine, the existence of errors in the lattice will decrease significantly the stable zone of the beam. The outer part of the beam may thus be destroyed, leading to possibility of escape for the particles in the non-definite torsion region, and the only usable part of the beam will remain the inner region with definite torsion. It is clear that in this case, all the efforts made in the design to avoid some resonant lines by bending the frequency map become totally vain.

Additionally, some analytical computation of the torsion could also be useful for the determination of the possible isotropic directions and the design of a lattice for which they are not harmful.

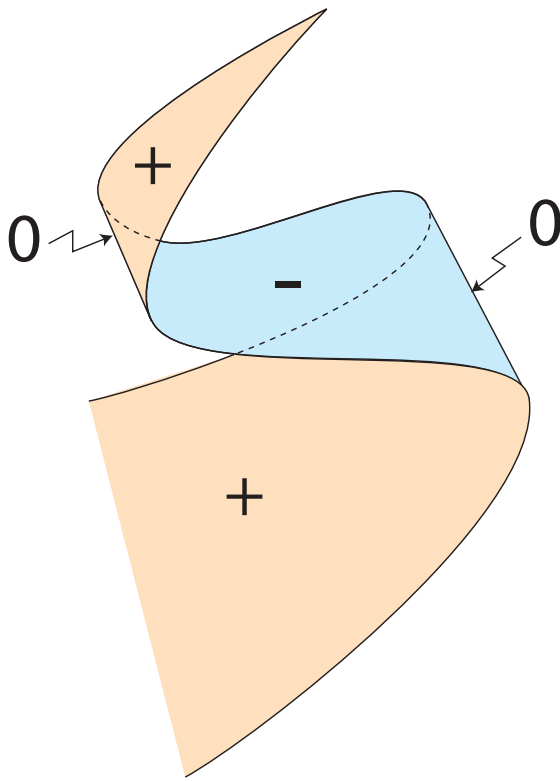


Figure 6: 2-folded frequency map.

## REFERENCES

[1] Laskar, J., The chaotic motion of the solar system. A numerical estimate of the size of the chaotic zones, *Icarus*, **88**, (266-291) (1990)

[2] Laskar, J., Froeschlé, C., Celletti, A., The measure of chaos by the numerical analysis of the fundamental frequencies. Application to the standard mapping, *Physica D*, **56**, (253-269) (1992)

[3] Laskar, J., Frequency analysis for multi-dimensional systems. Global dynamics and diffusion, *Physica D*, **67**, (257-281) (1993)

[4] Laskar, J., Robutel, P., The chaotic obliquity of the planets, *Nature*, **361**, (608-612) (1993)

[5] Von Milczewski, J., Farrelly, D. Uzer, T., Frequency Analysis of 3D Electronic  $1/r$  Dynamics: Tuning between Order and Chaos *Phys. Rev. Lett.*, **78**, 1436–1439 (1997)

[6] Papaphilippou, Y., Laskar, J., Frequency map analysis and global dynamics in a two degrees of freedom galactic potential, *Astron. Astrophys.*, **307**, (427-449) (1996)

[7] Papaphilippou, Y., Laskar, J., Global dynamics of triaxial galactic models through frequency map analysis, *Astron. Astrophys.*, **329**, (451-481) (1998)

[8] Valluri, M., Merritt, D., Regular and Chaotic Dynamics of Triaxial Stellar Systems *Astrophys. J.*, **506**, 686–711 (1998)

[9] Merritt, D., Valluri, M., Resonant Orbits in Triaxial Galaxies *Astron. J.*, **118**, 1177–1189 (1999)

[10] Wachlin, F. C.; Ferraz-Mello, S., Frequency map analysis of the orbital structure in elliptical galaxies *M.N.R.A.S.* **298**, 1, 22–32 (1998)

[11] Dumas, S., Laskar, J., Global Dynamics and Long-Time Stability in Hamiltonian Systems via Numerical Frequency

Analysis, *Phys. Rev. Lett.*, **70**, (2975-2979) (1993)

[12] Laskar, J., Robin, D., Application of frequency map analysis to the ALS, *Particle Accelerator*, **54**, (183-192) (1996)

[13] Robin, D., Steir, C., Laskar, J., Nadolski, L., Global dynamics of the ALS revealed through experimental Frequency Map Analysis, *Phys. Rev. Lett.*, **85**, pp. 558-561 (2000)

[14] Comunian, M., Pisent, A., Bazzani, A., Turchetti, G., Rambaldi, S.:2001, Frequency map analysis of a three-dimensional particle in the core model of a high intensity linac, *Phys. Rev. ST Accel. Beams* **4**, 124201 (2001)

[15] Papaphilippou, Y. Zimmermann, F., Weak-strong beam-beam simulations for the Large Hadron Collider, *Phys. Rev. ST Accel. Beams* **2**, 104001 (1999)

[16] Steier, C., Robin, D., Nadolski, L., Decking, W., Wu, Y., Laskar, J., Measuring and optimizing the momentum aperture in a particle accelerator, *Phys. Rev. E*, **65**, (056506) (2002)

[17] Nadolski, L., Laskar, J., Review of third generation light sources through frequency map analysis *Phys. Rev. E*, submitted (2003)

[18] Laskar, J., Frequency map analysis of an Hamiltonian system, Workshop on Nonlinear dynamics in particle accelerator, Arcidosso, 1994, AIP Conf. proc. **344**, S. Chattopadhyay, M. Cornacchia, C. Pellegrini, Eds, AIP Press, New York, pp 130–159 (1995)

[19] Laskar, J., Introduction to frequency map analysis, in *proc. of NATO ASI Hamiltonian Systems with Three or More Degrees of Freedom*, C. Simò ed, Kluwer, 134–150 (1999)

[20] Laskar, J., Frequency map analysis and quasiperiodic decompositions. preprint ([www.bdl.fr/Equipes/ASD/preprints/rep.2003/laskar\\_porq1.pdf](http://www.bdl.fr/Equipes/ASD/preprints/rep.2003/laskar_porq1.pdf)) (2003)

[21] Arnold, V.I., Kozlov, V.V., Neishtadt, A.I., Mathematical aspects of classical and celestial mechanics, *Dyn. Systems III*, V.I. Arnold, ed., Springer, New York. (1988)

[22] J. Pöschel, Integrability of Hamiltonian systems on Cantor sets, *Comm. Pure Appl. Math.*, **25**, 653–695 (1982)

[23] Robin, D., Safranek, J., Decking, W., Realizing the Benefits of restored Periodicity in the Advanced Light Source, *Phys. Rev. ST Accel. Beams*, **2**, 044001 (1999)

[24] Terebilo, A., Pellegrini, C., Cornacchia, M., Corbett, J., Martin, D., "Experimental non-linear beam dynamics studies at SPEAR", 1997 Particle Accelerator Conference, Vancouver, Canada, 1457 – 1459 (1998)

[25] Bartolini, R., Leunissen, L.H.A., Papaphilippou, Y., Schmidt, F., Verdier, A., "Measurement of resonance driving terms from turn-by-turn data", Particle Accelerator Conference, New York, 1557 - 1559 (1999)

[26] Papaphilippou, Y., Farvacque, L., Ropert, A., Laskar, J., Probing the non-linear dynamics of the ESRF storage ring with experimental frequency maps, PAC'03, Portland (2003)

[27] Belgroune, M., Brunelle, P., Laskar, J., Nadj, A., Application of the frequency map analysis to the new lattice of the SOLEIL project, EPAC2002 (2002)

[28] Nekhoroshev, N.N.:1977, An exponential estimates for the time of stability of nearly integrable Hamiltonian Systems, *Russian Math. Surveys*, **32**, 1–65 (and Niedermann, 2003, private communication)

[29] Arnold, V.I., Goryunov, V.V., Lyashko, O.V., Vasil'ev, V.A., Singularity theory I, *Dyn. Systems VI*, V.I. Arnold, ed., Springer, New York (1993)